

Circulating fluidized bed fly ash-derived mesoporous silica adsorbent for the adsorptive removal of malachite green

Ning Yuan*, Xinling Zhang, Licheng Sun, Shaoqing Liu, Dongmin Wang, Tao Zhu*

School of Chemical & Environmental Engineering, China University of Mining & Technology, Beijing 100083, China, emails: ning.yuan@hotmail.com (N. Yuan), bamboozt@cumt.edu.cn (T. Zhu), zhangxinling1215@foxmail.com (X. Zhang), 1696120012@qq.com (L. Sun), shaoqing134521@163.com (S. Liu), wangdongmin-2008@163.com (D. Wang)

Received 26 October 2018; Accepted 5 April 2019

ABSTRACT

An ordered mesoporous silica material of MCM-41 type (CFB-MS) was successfully fabricated from the circulating fluidized bed fly ash for the first time. CFB-MS was generally prepared through a two-step hydrothermal process, including the extraction of silicon from the raw material and the preparation of mesoporous adsorbent CFB-MS using the extracted supernatant. The mesostructure of the obtained CFB-MS was characterized by powder X-ray diffraction and nitrogen adsorption-desorption measurement, while its morphology was observed through transmission electron microscope. The chemical component of CFB-MS was confirmed via Fourier transform infrared spectroscopy, solid-state ^{29}Si and ^{27}Al MAS NMR spectroscopy. Furthermore, the adsorption behavior of malachite green (MG) onto CFB-MS was investigated by varying several influence factors, such as contact time, pH, dosage, initial concentration and temperature. Different adsorption isotherm and kinetic models were employed to fit the adsorption data to understand the adsorption process. It was found that the MG adsorption equilibrium followed Freundlich and Temkin isotherm models, while the adsorption process can be described through the pseudo-second-order kinetics model. In addition, the possible adsorption mechanisms were proposed to interpret the dye adsorption process. The present work provides a high-value utilization of circulating fluidized bed fly ash and a promising strategy for the removal of dye in aqueous solution.

Keywords: Circulating fluidized bed fly ash; MCM-41; Mesoporous material; Dye adsorption; Malachite green

1. Introduction

Varieties of dyes have been widely used in many industries, such as textile, dyeing, printing and food plants, and they have played a crucial role in contemporary society. However, untreated effluents from these industries contain significant amounts of dyes that are usually toxic and may cause severe environmental problems [1]. Furthermore, the color of dye wastewater is highly visible even at an extremely low concentration and thus is esthetically unpleasant [2]. Consequently, it is mandatory to purify the dye-containing wastewater prior to discharge into environment. Several

techniques have been proposed to the purification of wastewater based on physical, chemical and biological methods. Among these dye removal techniques, physical adsorption process has attracted considerable attention. It has been the major method used for modern industry because of its high efficiency and versatility [3]. A great variety of adsorbents, including activated carbons and zeolites, have been applied to the removal of dye during adsorption process until now [4,5]. However, their adsorption capacities for dyes are limited because of their microporous nature.

Alternatively, ordered mesoporous silica materials, first discovered by scientists in the Mobil Research and

* Corresponding authors.

Development Corporation (New Jersey, USA) [6], have also been applied to the treatment of contaminants in water because of their large specific area, tunable pore size and high stability [7]. Currently, the production of mesoporous silica was generally achieved by using commercial silica precursors such as tetraethyl orthosilicate, fumed silica and sodium metasilicate, which is not suitable for a large-scale production due to their relatively high cost [8,9]. Therefore, it is highly desirable to develop economical processes by utilizing cheaper silica sources in consideration of the large-scale industrial manufacture of mesoporous silica adsorbents [10,11].

On the other hand, coal-fired power plants around the world annually generate a great deal of industrial solid waste including fly ash and bottom ash. The consumption of these residues has drawn increasing concern because of not only their large amounts of production but also their serious influence on environment [12]. Generally, the fly ash has been consumed in building materials on a large scale during the past decades [13]. In order to achieve a high-value utilization, many scientists have made great efforts to realize the conversion of fly ashes into mesoporous silica materials due to the high content of useful silicon [14], and further investigated their applications in carbon dioxide capture [15], catalysis [16,17], removal of phosphate [18] and heavy metal ions [19]. For instance, Park et al. [15] used the bottom ash-derived mesoporous silica as support material for the impregnation of polyethyleneimine, and demonstrated that it possessed excellent capacity for carbon dioxide capture (218 mg g^{-1} at 75°C). Dhokte et al. [16] successfully prepared a MCM-41 material from the fly ash and utilized the obtained material as catalyst for the synthesis of β -amino carbonyl compounds via a classical Mannich reaction. However, only a very few fly ash-derived counterparts have been reported on the dye removal up to date [20]. Very recently, ordered mesoporous materials were synthesized and further evaluated as adsorbents for methylene blue removal by Zhou et al. [20]. Generally, the employment of fly ash-derived mesoporous silica materials for the dye removal is faintly developed and it can be a promising strategy for practical application.

With respect to the starting raw materials, the previous reports generally employed fly ashes generated by pulverized coal combustion to obtain mesoporous silica materials, and there is still no example of the synthesis of these porous materials using circulating fluidized bed fly ash. The latter raw material is produced through circulating fluidized bed combustion at lower temperature of 800°C – 950°C , and thus exhibits quite different components and morphology [21]. It is viewed that there exists more amorphous phase in circulating fluidized bed fly ash than in fly ash generated by pulverized coal combustion mainly due to different combustion temperatures [12]. Therefore, it is quite reasonable to utilize this kind of fly ash for the preparation of mesoporous silica molecular sieves.

Herein, the fabrication of mesoporous silica material from the circulating fluidized bed fly ash (CFB-MS) has been demonstrated in the present article for the first time. CFB-MS was synthesized through a two-step hydrothermal process and possessed a well-ordered MCM-41 mesostructure with hexagonal $p6mm$ symmetry. The structure and morphology of CFB-MS were characterized through powder X-ray

diffraction, nitrogen adsorption–desorption measurement, transmission electron microscopy (TEM), Fourier transform infrared spectroscopy (FT-IR), solid-state ^{29}Si and ^{27}Al MAS NMR spectroscopy. Furthermore, the adsorptive removal of a typical cationic dye, malachite green (MG), was investigated by varying several factors, including contact time, pH, dosage, initial concentration and temperature. In addition, the adsorption isotherm and kinetics were also studied in detail by applying different models in order to understand the adsorption mechanisms.

2. Experimental

2.1. Materials

The circulating fluidized bed fly ash used in the present study was obtained from an electric power plant in Shanxi, China. Concentrated hydrochloric acid (HCl, 36%–38%) and sulfuric acid (H_2SO_4 , 95%–98%) were purchased from the Sinopharm Chemical Reagent Co. Ltd., (Shanghai, China) Ammonium hydroxide ($\text{NH}_3\cdot\text{H}_2\text{O}$, 25%) and sodium hydroxide (NaOH) were bought from Beijing Chemical Works (Beijing, China) and Beijing Tong Guang Fine Chemicals Company (Beijing, China), respectively. Cetyltrimethylammonium bromide (CTAB) and malachite Green (MG) were from Tianjin Jinke Fine Chemical Research Institute (Tianjin, China) and Shanghai Maklin Biochemical Co. Ltd., (Shanghai, China), respectively. All chemicals were directly used without further purification. Deionized water used for all experiments was obtained from a water purification system in China University of Mining and Technology, Beijing, China.

2.2. Extraction of silicon from circulating fluidized bed fly ash

Before the extraction of silicon from circulating fluidized bed fly ash, a pre-treatment process was performed for the removal of impurities such as iron and calcium ions. Initially, the as-received circulating fluidized bed fly ash was dried in an oven at 100°C until no weight loss. Then, the dried starting material was added to 20% HCl and the mixture was stirred at 80°C for 4 h. After cooling to room temperature, the solid was separated from the solution by filtration and washed using deionized water for several times. Finally, the obtained solid was further dried in an oven at 100°C overnight.

The extraction of silicon was carried out under a hydrothermal condition. Specifically, the circulating fluidized bed fly ash after pre-treatment was mixed with NaOH solution of certain different concentration (2 – 5 mol L^{-1}) with a mass-to-volume ratio (g mL^{-1}) of 1:10. Thereafter, the obtained mixture was stirred at 80°C for 4 h. The supernatant was separated by centrifugation and filtration of the mixture. The silicon and aluminum concentrations of the obtained supernatant were detected by inductively coupled plasma optical emission spectrometry (ICP-OES) method.

2.3. Synthesis of mesoporous adsorbent CFB-MS

In a typical procedure for the synthesis of the mesoporous adsorbent, 1.2 g cetyltrimethylammonium bromide (CTAB) was added to a beaker containing 20 g deionized water and 1.0 g ammonium hydroxide ($\text{NH}_3\cdot\text{H}_2\text{O}$, 25%).

After being stirred at room temperature for 2 h, 30 mL of silicon-containing supernatant prepared from the circulating fluidized bed fly ash was dropped to the solution. After the mixture was further stirred for 2 h, the pH of the solution was adjusted to 10.0 by adding 5 mol L⁻¹ H₂SO₄ solution and stirred for another 30 min. Afterwards, the solution was transferred into an autoclave for hydrothermal treatment at 100°C for 48 h. The molar ratio of Si:CTAB:H₂O used here was 1:0.2:170. The as-synthesized adsorbent was recovered by centrifugation at 8,000 rpm and then fully washed by deionized water for several times. After being dried at 100°C in an oven overnight, the as-synthesized product was calcinated at 550°C for 6 h to remove the surfactant. Finally, a white powder denoted as CFB-MS was obtained.

2.4. Adsorption of malachite green

The adsorption process of MG onto the surface of CFB-MS was investigated by varying several factors including contact time, pH, dosage, initial concentration and temperature. In a typical procedure of adsorption process, CFB-MS fine powder (5 mg) and 200 mg L⁻¹ MG solution (10 mL) were successively added in a glass vial. Afterwards, the vial containing a mixture of adsorbent and dye solution was shaken in a shaker at 298 K for 40 min (150 rpm). CFB-MS was separated from the dye solution via centrifugation. Finally, the concentration of the supernatant containing the remained MG was determined through UV-Vis spectrophotometer at the calibrated maximum wavelength (λ_{\max}) of 620 nm.

The adsorption capacity (q_e) and removal efficiency (E) of MG onto CFB-MS were calculated by the following equations:

$$q_e = \frac{(C_0 - C_e)V}{m} \quad (1)$$

$$E = \frac{C_0 - C_e}{C_0} \times 100\% \quad (2)$$

where C_0 , C_e and q_e are initial concentration (mg L⁻¹), concentration at equilibrium (mg L⁻¹) and adsorption capacity at equilibrium (mg g⁻¹) for MG, respectively. In addition, m represents the amount of CFB-MS (g), and V stands for the volume of MG solution (L).

3. Results and discussion

3.1. Characterization of the circulating fluidized bed fly ash and CFB-MS

The chemical composition of the as-received circulating fluidized bed fly ash was analyzed by X-ray fluorescence (XRF), indicating that Si, Al, Ca and Fe were the major components. Table 1 summarizes the major components in oxide form, among which SiO₂ and Al₂O₃ account for weight percentages of 40.84 and 33.83, respectively.

The X-ray diffraction pattern of the as-received circulating fluidized bed fly ash is displayed in Fig. 1, which discloses that the major crystalline phases in the as-received starting material were quartz, anhydrite, calcite and mullite. Meanwhile, the broad band in 20°–30° suggests the presence of significant amount of amorphous matter. Generally,

Table 1
Chemical composition of as-received circulating fluidized bed fly ash used in this research

No.	Compound	Content (wt.%)	CFB (mol/100 g)
1	SiO ₂	40.84	0.680
2	Al ₂ O ₃	33.83	0.332
3	CaO	9.57	0.171
4	Fe ₂ O ₃	6.17	0.039
5	SO ₃	4.26	0.053
6	TiO ₂	1.81	0.023
7	MgO	1.04	0.026
8	CdO	0.94	0.007
9	K ₂ O	0.77	0.008
10	P ₂ O ₅	0.27	0.002
11	Na ₂ O	0.16	0.003
12	SrO	0.11	0.001

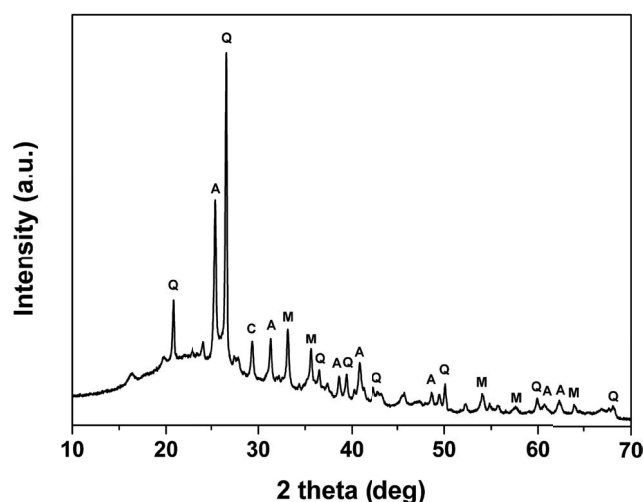


Fig. 1. X-ray diffraction pattern of the as-received circulating fluidized bed fly ash. Q: quartz (SiO₂), A: anhydrite (CaSO₄), C: calcite (CaCO₃), M: Mullite (3Al₂O₃·2SiO₂ or 2Al₂O₃·SiO₂).

amorphous components are favorable to be transformed into soluble sodium silicate during the hydrothermal treatment using NaOH, while crystalline phases are not easy to be converted into soluble sodium silicate [8]. Compared with pulverized coal furnace fly ash, more amorphous components exist in the circulating fluidized bed fly ash, thereby facilitating the extraction of silicon. Furthermore, the morphology of the as-received circulating fluidized bed fly ash was revealed by TEM. Fig. S1 exhibits an irregular particle shape, which is quite different from pulverized coal furnace fly ash featuring the presence of spherical particles because of the different combustion temperatures [21].

The silicon and aluminum concentrations of the supernatant extracted from circulating fluidized bed fly ash were analyzed by inductively coupled plasma optical emission spectrometry (ICP-OES) method. The results are plotted in Fig. 2. When varying the concentration of NaOH solution from 2 to 5 mol L⁻¹, the extracted silicon concentration

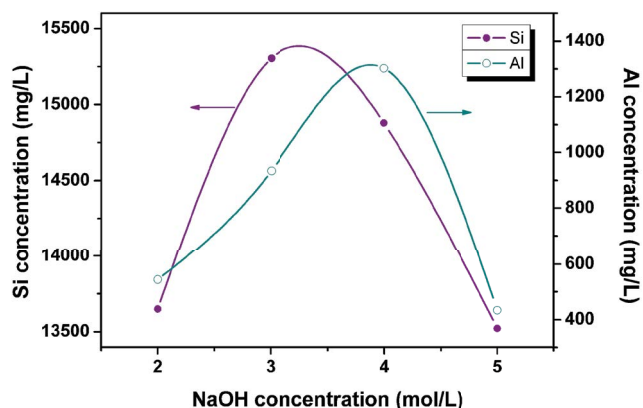


Fig. 2. Curves of the silicon and aluminum concentrations of the supernatant extracted from the circulating fluidized bed fly ash under different concentrations of NaOH solution.

increased from 13,650 to 15,305 ppm (at 3 mol L⁻¹ NaOH), and then decreased to 13,523 ppm. A similar trend was found for the extracted aluminum concentration with a summit of 1,303 ppm at the NaOH concentration of 4 mol L⁻¹. To employ the silicon for the fabrication of mesoporous silica adsorbent, the NaOH concentration was set at 3 mol L⁻¹ for the extraction of silicon from circulating fluidized bed fly ash.

The low-angle powder X-ray diffraction was employed to examine the structural ordering of the circulating fluidized bed fly ash-derived mesoporous silica material, namely CFB-MS. As shown in Fig. 3, CFB-MS exhibits four clearly resolved diffraction peaks which can be indexed as (100), (110), (200) and (210) reflections of MCM-41 with p6mm symmetry, respectively. The pore structure parameter (a_0) was calculated to be 4.64 nm based on the equation $a_0 = 2d_{100} / \sqrt{3}$, and the thickness of the pore wall (w_p) was 1.90 nm according to the equation $w_p = a_0 - d_p$, where d_p is the maximum value of BJH pore size distribution from desorption branch [22].

Nitrogen adsorption–desorption measurements were further carried out to investigate the textural properties of CFB-MS. As displayed in Fig. 4a, CFB-MS possesses a characteristic type IV isotherm according to IUPAC nomenclature with hysteresis loop, indicative of the presence of mesoporous structure [23]. Results from nitrogen adsorption–desorption isotherm are in agreement with that of the low-angle XRD. The Brunauer–Emmett–Teller (BET) specific surface area and pore volume of CFB-MS were calculated to be 738 m² g⁻¹ and 0.66 cm³ g⁻¹, respectively. The BET specific surface area and pore volume of CFB-MS were comparable to that of the previously reported MCM-41 materials prepared from pulverized coal furnace fly ash [8–11,17,24]. The BET specific surface area of CFB-MS presented here was higher than that of the MCM-41 material derived from coal fly ash (525 m² g⁻¹) for dye removal very recently [20]. Furthermore, the corresponding pore diameter was evaluated through the desorption branch of isotherm by applying the Barrett–Joyner–Halenda (BJH) model. As shown in Fig. 4b, CFB-MS exhibited relatively narrow pore size distribution around 2.74 nm, and the average pore diameter was calculated to be 3.22 nm.

The morphology of the circulating fluidized bed fly ash-derived MCM-41 type mesoporous silica material

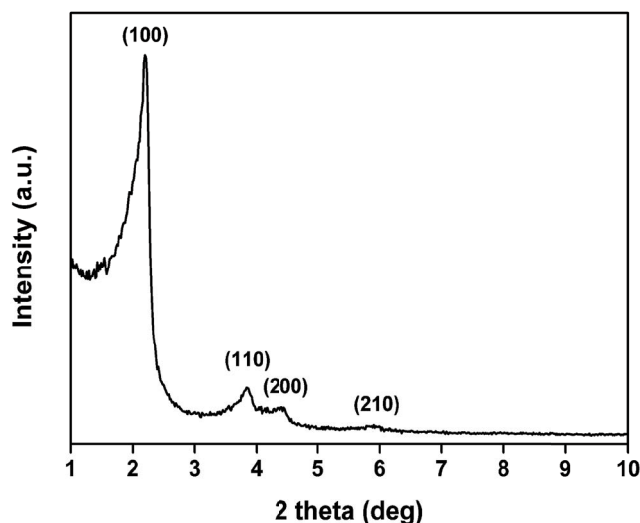


Fig. 3. Powder X-ray diffraction pattern of CFB-MS.

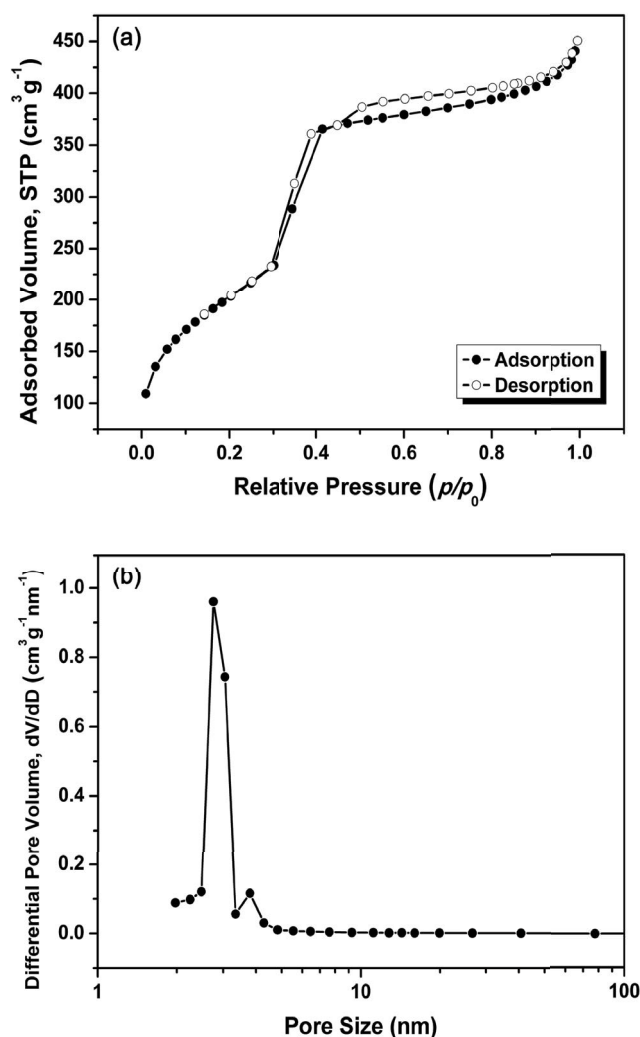


Fig. 4. Nitrogen adsorption–desorption isotherm (a) and pore size distribution curve (b) of the obtained adsorbent CFB-MS.

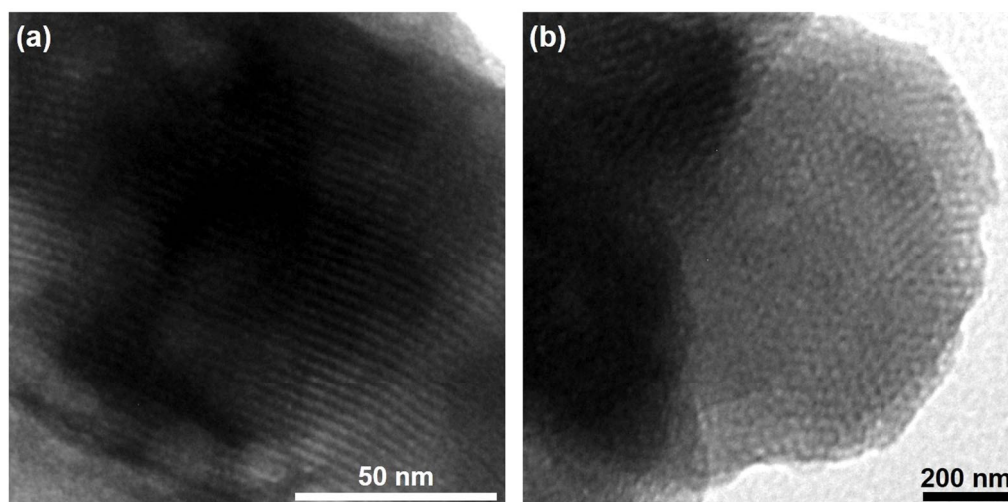


Fig. 5. TEM images of the obtained CFB-MS material.

(CFB-MS) was observed by TEM. As expected, CFB-MS exhibits well-ordered one-dimensional arrays of uniform mesopores (Fig. 5), which is characteristic of a hexagonal $p6mm$ mesostructure and consistent with the results inferred from the low-angle powder X-ray diffraction and nitrogen physisorption measurement.

The chemical component of CFB-MS was further confirmed by FT-IR. As depicted in Fig. 6, the broad absorption band around $3,457\text{ cm}^{-1}$ corresponds to O–H stretching vibrations of the surface silanol groups and water molecules [25]. The intense absorption peak at $1,107\text{ cm}^{-1}$ can be attributed to asymmetry stretching vibration of T–O–T bond (T represents Si or Al), which displays a shift to lower wavenumber in comparison with the asymmetry stretching vibration of Si–O–Si bond of pure silica MCM-41 [26]. The decrease in wavenumber was due to the substitution of silicon by a larger-sized metal ion, that is, aluminum [26]. The peaks emerged at 800 and 470 cm^{-1} can be assigned to symmetric stretching and deformation vibrations of T–O–T bond (T represents Si or Al), respectively [16]. In addition, an absorption peak appearing at $1,632\text{ cm}^{-1}$ is characteristic of deformation vibration of the physically adsorbed water molecules. Therefore, FT-IR spectrum demonstrates the successful fabrication of aluminosilicate framework within CFB-MS prepared from circulating fluidized bed fly ash.

Solid-state ^{29}Si MAS NMR spectroscopy was adopted to check the chemical state of silicon atoms in CFB-MS. As shown in Fig. 7a, the peak signals at -109.2 , -99.1 and -91.3 ppm are attributed to Q^n ($Q^n = \text{Si}(\text{OSi})_n(\text{OH})_{4-n}$, $n = 4, 3$ and 2) [8,22,25]. Furthermore, ^{27}Al MAS NMR spectrum for CFB-MS was also measured in order to investigate the chemical state of aluminum within the obtained material. The spectrum displays a very strong resonance at ca. 54.1 ppm , which is corresponding to tetrahedral coordination of aluminum in the framework [10]. In addition, no peak assigned to octahedral non-framework aluminum at 0 ppm was observed. These findings suggest that silicon and aluminum sources in the supernatant extracted from circulating fluidized bed fly ash have been successfully incorporated in the framework of CFB-MS.

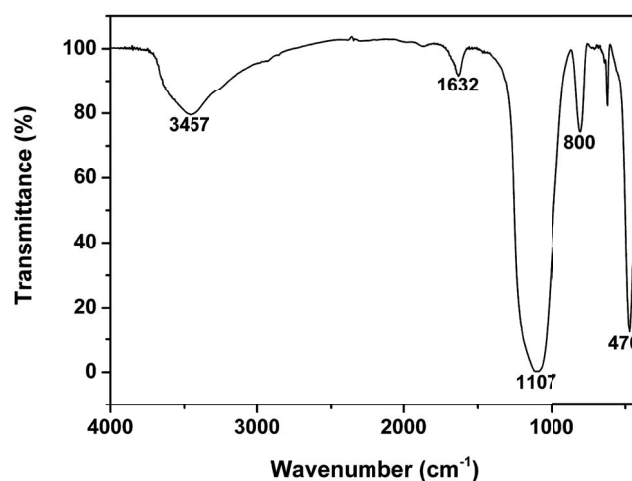


Fig. 6. Fourier transform infrared spectrum of CFB-MS.

3.2. Methylene blue adsorption

3.2.1. Effects of factors on adsorption

To investigate the effect of contact time on the adsorption process, the obtained CFB-MS (5 mg) was added to 10 mL MG solution with initial concentration of 200 mg L^{-1} by changing the contact time from 2 to 240 min (Fig. 8a). It can be observed that adsorption amount increases rapidly with the increase in contact time at this early stage. After 20 min , the uptake capacity reaches the maximum of 258.61 mg g^{-1} , and remains almost constant when the contact time is further increased, indicative of the advent of adsorption equilibrium. By comparison with the previously reported mesoporous silica adsorbents, CFB-MS exhibits a competitive adsorption capacity and a shorter adsorption equilibrium time. The short equilibrium time suggests that the large-sized and ordered mesopores within the CFB-MS adsorbent are favorable to fast mass transfer of MG molecules. In addition, the high initial MG concentration and the abundant vacant adsorption sites in CFB-MS also contribute

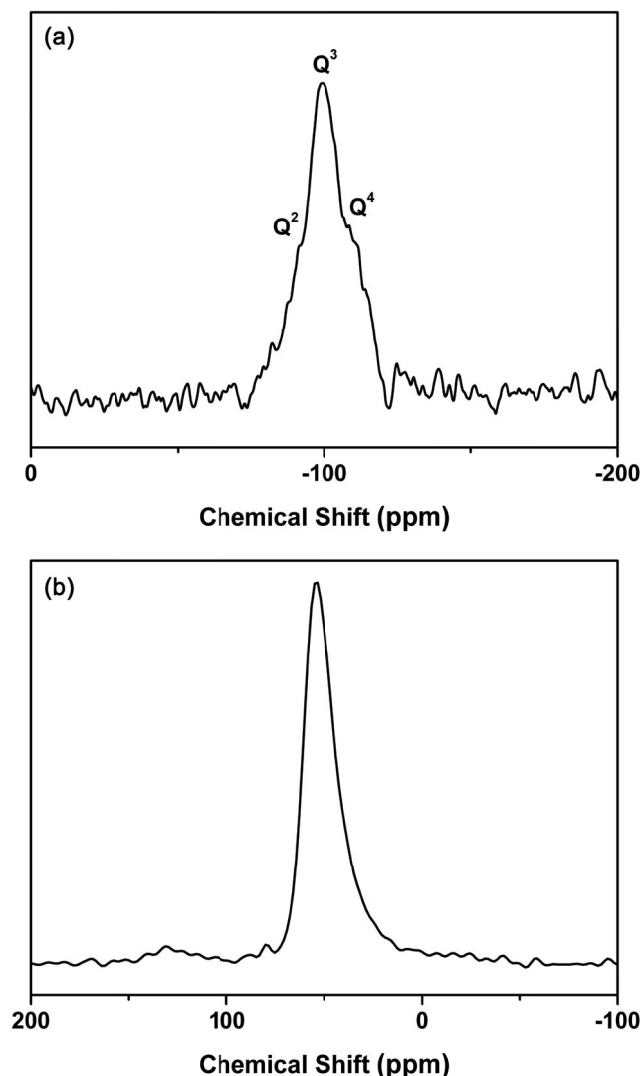


Fig. 7. Solid-state ^{29}Si (a) and ^{27}Al MAS NMR spectra (b) of the synthesized CFB-MS material.

the relatively high adsorption capacity and short equilibrium adsorption time.

The initial pH of the solution can significantly influence the degree of ionization of MG and the surface charge of the CFB-MS adsorbent, thereby altering the adsorption process and particularly adsorption amount. In this research, the initial pH is set ranging from 3 to 10. It can be found that the adsorption amount increased gradually when increasing the pH of MG solution, and the maximum adsorption amount occurred at pH of 10 as depicted in Fig. 8b. This trend can be probably interpreted by the electrostatic interactions between MG and CFB-MS. As a cationic dye, MG favors negatively charged surface sites. Therefore, more silanol groups Si-OH on the adsorbent surface will be deprotonated and displays the formation of Si-O⁻ with increasing pH of the solution, which thus exhibits enhanced electrostatic interaction with the cationic dye MG. Results reported here are also in accordance with the related previous works [20,27].

The effect of CFB-MS dosage on the adsorption amount of MG from aqueous solution has been investigated by dispersing different amount of CFB-MS from 3 to 24 mg into 10 mL of 200 mg L⁻¹ MG solution at 298 K and the optimum pH 10. As presented in Fig. 8c, the adsorption amount decreases with the increase in dosage of CFB-MS, in which the maximum adsorption amount is found to be 286.85 mg g⁻¹ at the dosage of 3 mg (i.e., 0.3 g L⁻¹). This indicates that a higher affinity of adsorbent for MG can be achieved at a relatively low dosage of CFB-MS [28–30]. A lower dosage means that less adsorbent surface is exposed to more dye molecules per gram unit of CFB-MS, and hence results in a high adsorption amount [31]. In addition, the available adsorption sites are probably unsaturated for MG molecules when increasing the dosage of CFB-MS [32].

The initial concentration of MG solution possesses great influence on the removal efficiency. In the present study, the initial concentration of MG solution is varied in the range of 25–200 mg L⁻¹ at three different temperatures, that is, 298, 308 and 318 K. It is observed that the removal efficiency increases gradually and then remains almost constant with increasing the initial MG concentration at these three different temperatures, as depicted in Fig. 8d. The equilibrium adsorption capacity increases linearly with the increase in initial MG concentration (Fig. S2). This is because that the increase in initial MG concentration could lead to an increase in the driving force of the concentration gradient [31]. Meanwhile, temperature also shows significant effect on the adsorption process. For each initial concentration, evaluating the temperature generally gave rise to the enhanced removal efficiency, indicating an endothermic nature of adsorption process [27,33]. Therefore, the adsorption process may undergo a chemical process [34]. This similar behavior was also revealed by previous literature [27,33,34].

3.2.2. Adsorption isotherms

Adsorption isotherms are commonly used to assess the distribution of solute between the adsorbent and solution. In this study, the Langmuir, Freundlich and Temkin isotherm models have been applied to the adsorption system. The isotherms have been investigated at three temperatures, that is, 298, 308 and 318 K.

The Langmuir isotherm [35–37] assumes that the adsorption of adsorbate takes place at specific homogeneous sites of the adsorbent surface. The Langmuir isotherm equation can be given as follows:

$$\frac{C_e}{q_e} = \frac{1}{k_L q_m} + \frac{C_e}{q_m} \quad (3)$$

where q_e and q_m represent the adsorption amounts (mg g⁻¹) at equilibrium and the maximum adsorption amounts (mg g⁻¹) of MG onto CFB-MS, respectively, C_e is the equilibrium concentration of MG solution (mg L⁻¹), and k_L stands for the Langmuir isotherm constant (L mg⁻¹) that is related to energy of adsorption.

As an empirical equation, the Freundlich isotherm [38,39] depicts that the adsorption can occur at heterogeneous sites within the adsorbent surface and may form either monolayer

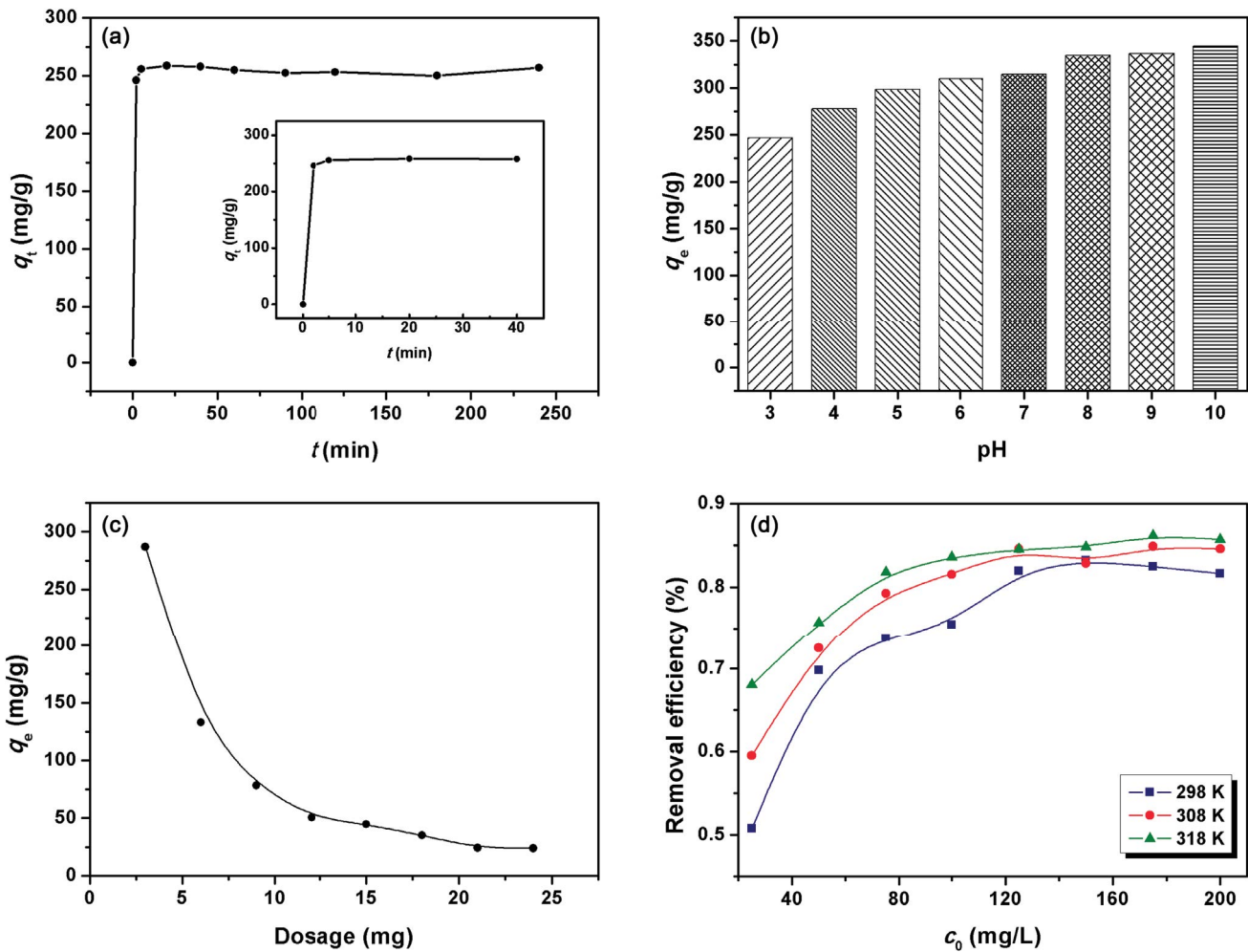


Fig. 8. Effects of contact time (a), pH (b), dosage (c), initial concentration and temperature (d) and on the adsorption amount of MG onto CFB-MS at 298 K.

or multilayer. The Freundlich isotherm equation can be described as:

$$\log q_e = \frac{1}{n} \log C_e + \log k_f \quad (4)$$

where k_f stands for the Freundlich adsorption constant ($(\text{mg g}^{-1}) (\text{mg L}^{-1})^{-1/n}$) that is related to adsorption capacity, and $1/n$ represents the adsorption intensity and surface heterogeneity.

The Temkin adsorption isotherm theory [40,41] takes into account the interactions between adsorbent and adsorbate. Furthermore, it assumes that the heat of adsorption of all molecules in the layer decreases linearly with increasing the surface coverage. The linear form of Temkin isotherm equation can be written as Eq. (5):

$$q_e = \frac{RT}{b_T} \ln C_e + \frac{RT}{b_T} \ln k_T \quad (5)$$

$$B_T = \frac{RT}{b_T} \quad (6)$$

where k_T represents the Temkin isotherm constant (L g^{-1}), b_T is a constant related to the heat of adsorption, R is universal gas constant ($8.314 \text{ J mol}^{-1} \text{ K}^{-1}$) and T is absolute temperature in Kelvin.

The linear forms of three types of isotherms are plotted in Fig. 9, and the corresponding parameters are presented in Table 2. Based on the linear regression coefficients (R^2), chi-squares (χ^2 , Eq. (7)) and root mean square errors (RMSE, Eq. (8)), it can be found that Freundlich and Temkin models give more appropriate fit to the isotherm data than the Langmuir isotherm model, indicating that the removal of MG occurs at heterogeneous adsorption sites and there exists interactions between MG and CFB-MS. Due to the positive value of b_T that is related to the heat of adsorption, the adsorption process of MG onto CFB-MS is exothermic. Furthermore, the high B_T values suggest that the interactions between MG onto CFB-MS are very strong [31].

$$\chi^2 = \sum_{i=1}^n \frac{(q_{e,\text{exp}} - q_{e,\text{cal}})^2}{q_{e,\text{exp}}^2} \quad (7)$$

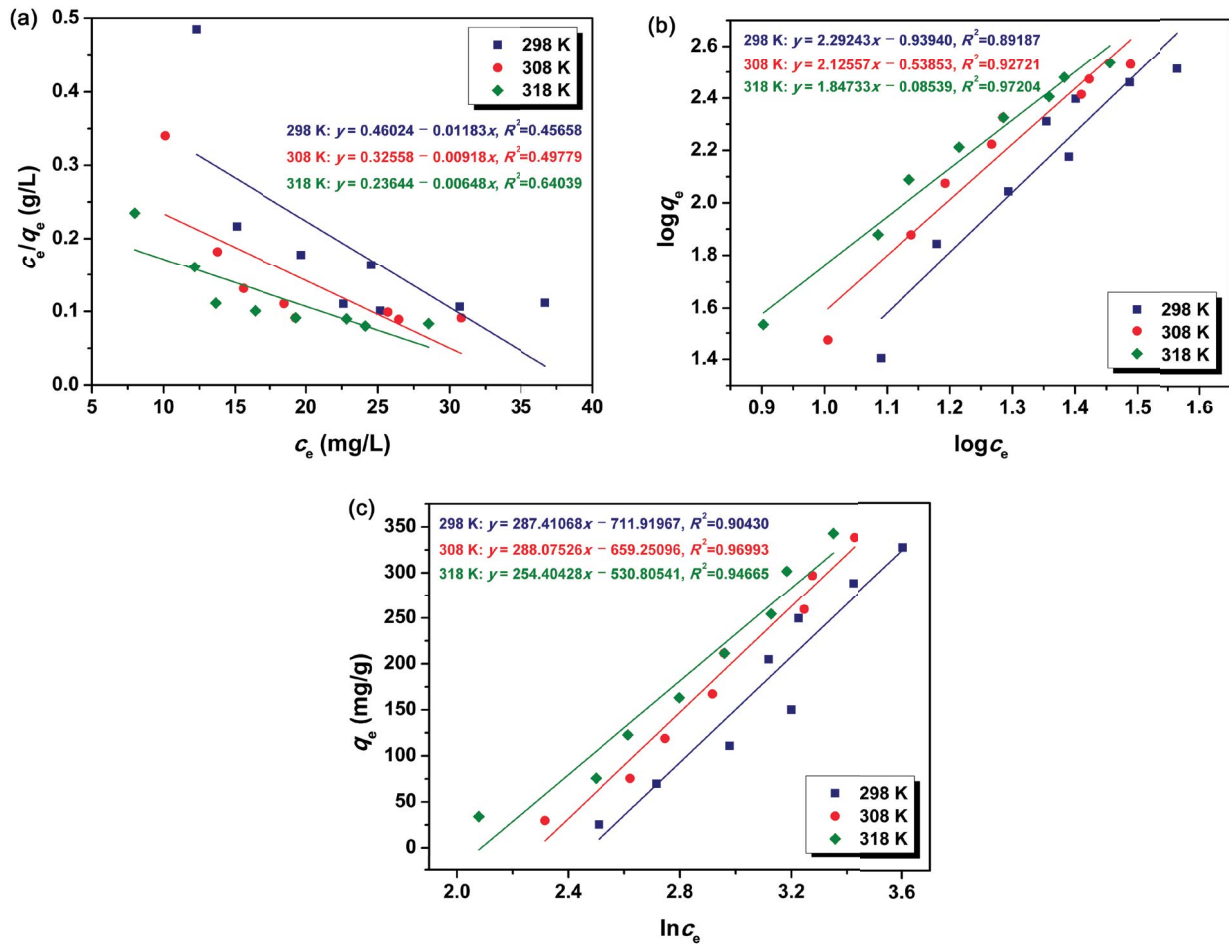


Fig. 9. Langmuir (a), Freundlich (b) and Temkin (c) adsorption isotherms fitted to the adsorption equilibrium data in linear forms for CFB-MS.

Table 2
Isotherms parameters for MG adsorption on obtained adsorbent CFB-MS

Isotherms	Parameters	Temperatures		
		298 K	308 K	318 K
Langmuir	q_m (mg g ⁻¹)	-84.53	-108.93	-154.32
	k_L (L mg ⁻¹)	-0.026	-0.028	-0.027
	R^2	0.45658	0.49779	0.64039
	χ^2	3,690.59	496.12	155.07
	RMSE	446.00	161.75	89.73
Freundlich	k_f ((mg g ⁻¹) (mg L ⁻¹) ^{-1/n})	0.11	0.29	0.82
	n	0.44	0.47	0.54
	R^2	0.89187	0.92721	0.97204
	χ^2	86.37	48.74	18.52
	RMSE	60.79	44.82	27.87
Temkin	b_T	8.62	8.89	10.39
	k_T (L g ⁻¹)	0.084	0.101	0.124
	R^2	0.90430	0.96993	0.94665
	χ^2	50.11	28.17	56.75
	RMSE	33.17	18.89	25.17

$$RMSE = \sqrt{\frac{1}{n-2} \sum_{i=1}^n (q_{e,exp} - q_{e,cal})^2} \quad (8)$$

3.2.3. Adsorption kinetics

The adsorption kinetics have also been investigated to better understand the rate and mechanism of MG adsorption onto CFB-MS. In the present work, the pseudo-first-order and pseudo-second-order kinetics models have been employed to evaluate the mass transfer process. The linear form of pseudo-first-order model was described by Lagergren [42] as shown in Eq. (9), and the pseudo-second-order model with linear form proposed by Ho and McKay [43] can be represented in Eq. (10):

$$\ln(q_e - q_t) = \ln q_e - k_1 t \quad (9)$$

$$\frac{t}{q_t} = \frac{1}{k_2 q_e^2} + \frac{t}{q_e} \quad (10)$$

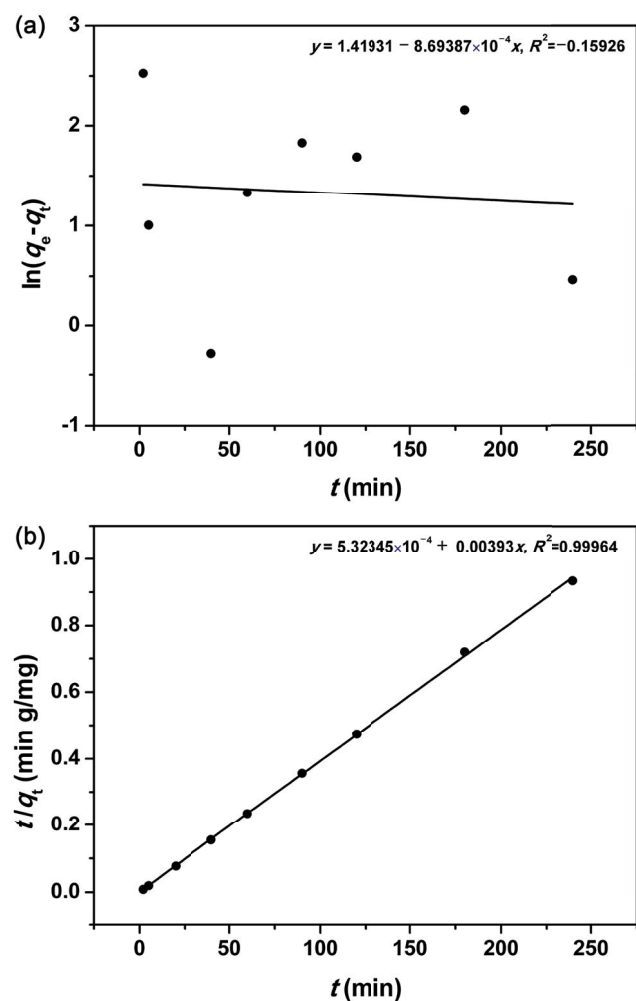


Fig. 10. Plots of the pseudo-first-order (a) and pseudo-second-order (b) kinetic models for MG adsorption onto CFB-MS.

where q_e and q_t stand for adsorption amounts (mg g^{-1}) of MG on CFB-MS at equilibrium and at time t (min), respectively. Meanwhile, k_1 (min^{-1}) and k_2 ($\text{g mg}^{-1} \text{min}^{-1}$) represent equilibrium rate constants of pseudo-first-order and pseudo-second-order kinetic models, respectively.

The kinetics models with linear form are plotted in Fig. 10, and the values of q_e , k_1 , k_2 and R^2 are summarized in Table 3. By comparison with correlation coefficients (R^2), it can be concluded that the adsorption of MG onto CFB-MS can be better described by pseudo-second-order kinetics model ($R^2 = 0.9996$) on the assumption that the rate limiting step involves chemisorption of the adsorbate onto the adsorbent. Moreover, the calculated uptake amount at equilibrium (254.45 mg g^{-1}) deduced from pseudo-second-order kinetics model is almost in accordance with the experimental value (258.61 mg g^{-1}).

3.2.4. Adsorption mechanism

The adsorption of malachite green (MG) onto the surface of CFB-MS can be interpreted by electrostatic interaction, hydrogen bonding and coordination between aluminum and nitrogen donor of MG molecule. As illustrated in Fig. 11, the adsorption can mainly attribute to the electrostatic interaction between cationic MG and the deprotonated adsorbent surface at high pH with the formation of T-O⁻ (T stands for Si or Al). Besides, the hydrogen bonding between the nitrogen donor of amine group within MG molecule and

Table 3
Parameters of pseudo-first-order and pseudo-second-order adsorption kinetics models

Kinetics models	Parameters	
Pseudo-first-order	$q_{e,cal}$ (mg g^{-1})	4.13
	k_1 (min^{-1})	8.69×10^{-4}
	R^2	-0.1593
Pseudo-second-order	$q_{e,cal}$ (mg g^{-1})	254.45
	k_2 ($\text{g mg}^{-1} \text{min}^{-1}$)	2.90×10^{-2}
	R^2	0.9996

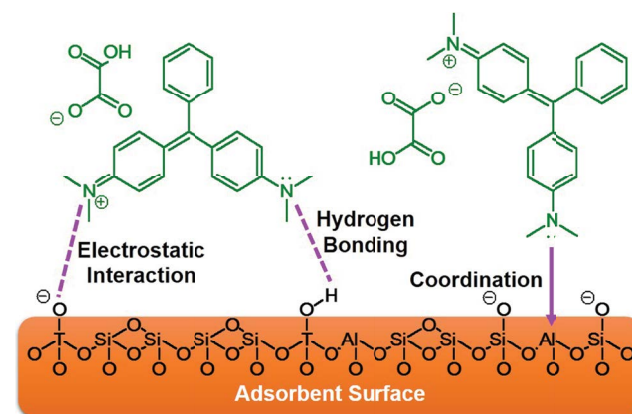


Fig. 11. Possible adsorption mechanisms of MG onto CFB-MS, where T represents Si or Al.

T–OH of the adsorbent surface is probably also responsible for the MG adsorption [44]. In addition, owing to the presence of Lewis acid site aluminum that was incorporated in the adsorbent CFB-MS as revealed by solid-state ^{27}Al MAS NMR spectrum, the coordination of aluminum with nitrogen donor of MG molecule also contributes to the adsorption [20]. Consequently, the adsorption mechanisms could be explained by electrostatic interaction, hydrogen bonding and metal coordination.

4. Conclusions

An ordered mesoporous silica sieve (CFB-MS) has been successfully prepared by using the circulating fluidized bed fly ash from coal-fired power plants. It represents the first example of the conversion of circulating fluidized bed fly ash into mesoporous silica materials. The obtained CFB-MS has been characterized by powder X-ray diffraction, nitrogen adsorption–desorption measurement, TEM, FT-IR and solid-state ^{29}Si and ^{27}Al MAS NMR spectroscopy. CFB-MS exhibits the mesostructure of MCM-41 with $p6mm$ symmetry, and possesses relatively large BET specific area and high pore volume of $738\text{ m}^2\text{ g}^{-1}$ and $0.66\text{ cm}^3\text{ g}^{-1}$, respectively. Several influence factors, including contact time, pH, dosage, initial concentration and temperature, have been investigated to evaluate its adsorptive removal efficiency of malachite green. It can be found that Freundlich and Temkin models give more appropriate fit to the isotherm data than the Langmuir isotherm model, while the adsorption of MG onto CFB-MS can be better described by pseudo-second-order kinetics model.

Acknowledgments

This work was supported by the Major Science and Technology Projects of Shanxi Province (20181102017) and the Fundamental Research Funds for the Central Universities (2017QH01).

References

- [1] M.T. Yagub, T.K. Sen, S. Afroze, H.M. Ang, Dye and its removal from aqueous solution by adsorption: a review, *Adv. Colloid Interface Sci.*, 209 (2014) 172–184.
- [2] Q. Qin, J. Ma, K. Liu, Adsorption of anionic dyes on ammonium-functionalized MCM-41, *J. Hazard. Mater.*, 162 (2009) 133–139.
- [3] Z. Cai, Y. Sun, W. Liu, F. Pan, P. Sun, J. Fu, An overview of nanomaterials applied for removing dyes from wastewater, *Environ. Sci. Pollut. Res.*, 24 (2017) 15882–15904.
- [4] A.R. Cestari, E.F.S. Vieira, G.S. Vieira, L.P. da Costa, A.M.G. Tavares, W. Loh, C. Airoidi, The removal of reactive dyes from aqueous solutions using chemically modified mesoporous silica in the presence of anionic surfactant—The temperature dependence and a thermodynamic multivariate analysis, *J. Hazard. Mater.*, 161 (2009) 307–316.
- [5] Y. Zhang, Z.-A. Qiao, Y. Li, Y. Liu, Q. Huo, Cooperative adsorbent based on mesoporous SiO_2 for organic pollutants in water, *J. Mater. Chem.*, 21 (2011) 17283.
- [6] C.T. Kresge, M.E. Leonowicz, W.J. Roth, J.C. Vartuli, J.S. Beck, Ordered mesoporous molecular sieves synthesized by a liquid-crystal template mechanism, *Nature*, 359 (1992) 710–712.
- [7] L.T. Gibson, Mesosilica materials and organic pollutant adsorption: part B removal from aqueous solution, *Chem. Soc. Rev.*, 43 (2014) 5173–5182.
- [8] M. Halina, S. Ramesh, M.A. Yarmo, R.A. Kamarudin, Non-hydrothermal synthesis of mesoporous materials using sodium silicate from coal fly ash, *Mater. Chem. Phys.*, 101 (2007) 344–351.
- [9] H. Misran, R. Singh, S. Begum, M.A. Yarmo, M. Ambar, Processing of mesoporous silica materials (MCM-41) from coal fly ash, *J. Mater. Process. Technol.*, 186 (2007) 8–13.
- [10] P. Kumar, N. Mal, Y. Oumi, K. Yamana, T. Sano, Mesoporous materials prepared using coal fly ash as the silicon and aluminium source, *J. Mater. Chem.*, 11 (2001) 3285–3290.
- [11] G. Chandrasekar, K.-S. You, J.-W. Ahn, W.-S. Ahn, Synthesis of hexagonal and cubic mesoporous silica using power plant bottom ash, *Microporous Mesoporous Mater.*, 111 (2008) 455–462.
- [12] J. Ding, S. Ma, S. Shen, Z. Xie, S. Zheng, Y. Zhang, Research and industrialization progress of recovering alumina from fly ash: a concise review, *Waste Manage.*, 60 (2017) 375–387.
- [13] R.S. Blissett, N.A. Rowson, A review of the multi-component utilisation of coal fly ash, *Fuel*, 97 (2012) 1–23.
- [14] Y.-R. Lee, J.T. Soe, S. Zhang, J.-W. Ahn, M.B. Park, W.-S. Ahn, Synthesis of nanoporous materials via recycling coal fly ash and other solid wastes: a mini review, *Chem. Eng. J.*, 317 (2017) 821–843.
- [15] J.-E. Park, H.-K. Youn, S.-T. Yang, W.-S. Ahn, CO_2 capture and MWCNTs synthesis using mesoporous silica and zeolite 13X collectively prepared from bottom ash, *Catal. Today*, 190 (2012) 15–22.
- [16] A.O. Dhokte, S.L. Khillare, M.K. Lande, B.R. Arbad, Synthesis, characterization of mesoporous silica materials from waste coal fly ash for the classical Mannich reaction, *J. Ind. Eng. Chem.*, 17 (2011) 742–746.
- [17] Y. Zhang, L. Kang, J. Shang, H. Gao, A low cost synthesis of fly ash-based mesoporous nanocomposites for production of hydrogen by photocatalytic water-splitting, *J. Mater. Sci.*, 48 (2013) 5571–5578.
- [18] D. Li, H. Min, X. Jiang, X. Ran, L. Zou, J. Fan, One-pot synthesis of Aluminum-containing ordered mesoporous silica MCM-41 using coal fly ash for phosphate adsorption, *J. Colloid Interface Sci.*, 404 (2013) 42–48.
- [19] G. Qi, X. Lei, L. Li, Y. Sun, C. Yuan, B. Wang, L. Yin, H. Xu, Y. Wang, Coal fly ash-derived mesoporous calcium-silicate material (MCSM) for the efficient removal of Cd(II), Cr(III), Ni(II) and Pb(II) from acidic solutions, *Procedia Environ. Sci.*, 31 (2016) 567–576.
- [20] C. Zhou, Q. Gao, W. Luo, Q. Zhou, H. Wang, C. Yan, P. Duan, Preparation, characterization and adsorption evaluation of spherical mesoporous Al-MCM-41 from coal fly ash, *J. Taiwan Inst. Chem. Eng.*, 52 (2015) 147–157.
- [21] Q.-c. Yang, S.-h. Ma, S.-l. Zheng, R. Zhang, Recovery of alumina from circulating fluidized bed combustion Al-rich fly ash using mild hydrochemical process, *Trans. Nonferrous Met. Soc. China*, 24 (2014) 1187–1195.
- [22] N. Yuan, Y. Liang, E.S. Erichsen, R. Anwander, Lanthanide complex-incorporated periodic mesoporous organosilica nanospheres with tunable photoluminescence, *RSC Adv.*, 5 (2015) 83368–83376.
- [23] M. Thommes, K. Kaneko, A. V. Neimark, J.P. Olivier, F. Rodriguez-Reinoso, J. Rouquerol, K.S.W. Sing, Physisorption of gases, with special reference to the evaluation of surface area and pore size distribution (IUPAC Technical Report), *Pure Appl. Chem.*, 87 (2015) 1051–1069.
- [24] M. Sari Yilmaz, N. Karamahmut Mermer, Conversion of fly ashes from different regions to mesoporous silica: effect of the mineralogical composition, *J. Sol-Gel Sci. Technol.*, 78 (2016) 239–247.
- [25] N. Yuan, Z.W. Liu, L.Y. Wang, B.H. Han, Rattle-type diamine-functionalized mesoporous silica sphere for carbon dioxide adsorption, *J. Nano Res.*, 53 (2018) 13–21.
- [26] K.S. Hui, C.Y.H. Chao, Synthesis of MCM-41 from coal fly ash by a green approach: Influence of synthesis pH, *J. Hazard. Mater.*, 137 (2006) 1135–1148.
- [27] M. Anbia, S.A. Hariri, Removal of methylene blue from aqueous solution using nanoporous SBA-3, *Desalination*, 261 (2010) 61–66.
- [28] N.M. Mahmoodi, S. Khorramfar, F. Najafi, Amine-functionalized silica nanoparticle: preparation, characterization and anionic dye removal ability, *Desalination*, 279 (2011) 61–68.
- [29] F. Chen, E. Zhao, T. Kim, J. Wang, G. Hableel, P.J.T. Reardon, S.J. Ananthakrishna, T. Wang, S. Arconada-Alvarez, J.C. Knowles,

- J.V. Jokerst, Organosilica nanoparticles with an intrinsic secondary amine: an efficient and reusable adsorbent for dyes, *ACS Appl. Mater. Interfaces*, 9 (2017) 15566–15576.
- [30] M. Anbia, S. Salehi, Removal of acid dyes from aqueous media by adsorption onto amino-functionalized nanoporous silica SBA-3, *Dyes Pigm.*, 94 (2012) 1–9.
- [31] A.H. Karim, A.A. Jalil, S. Triwahyono, S.M. Sidik, N.H.N. Kamarudin, R. Jusoh, N.W.C. Jusoh, B.H. Hameed, Amino modified mesostructured silica nanoparticles for efficient adsorption of methylene blue, *J. Colloid Interface Sci.*, 386 (2012) 307–314.
- [32] A.A. Jalil, S. Triwahyono, S.H. Adam, N.D. Rahim, M.A.A. Aziz, N.H.H. Hairom, N.A.M. Razali, M.A.Z. Abidin, M.K.A. Mohamadiah, Adsorption of methyl orange from aqueous solution onto calcined Lapindo volcanic mud, *J. Hazard. Mater.*, 181 (2010) 755–762.
- [33] H. Chaudhuri, S. Dash, A. Sarkar, SBA-15 functionalised with high loading of amino or carboxylate groups as selective adsorbent for enhanced removal of toxic dyes from aqueous solution, *New J. Chem.*, 40 (2016) 3622–3634.
- [34] R. Han, J. Zhang, P. Han, Y. Wang, Z. Zhao, M. Tang, Study of equilibrium, kinetic and thermodynamic parameters about methylene blue adsorption onto natural zeolite, *Chem. Eng. J.*, 145 (2009) 496–504.
- [35] I. Langmuir, The constitution and fundamental properties of solids and liquids. Part I. Solids, *J. Am. Chem. Soc.*, 38 (1916) 2221–2295.
- [36] I. Langmuir, The constitution and fundamental properties of solids and liquids. II. Liquids, *J. Am. Chem. Soc.*, 39 (1917) 1848–1906.
- [37] I. Langmuir, The adsorption of gases on plane surfaces of glass, mica and platinum, *J. Am. Chem. Soc.*, 40 (1918) 1361–1403.
- [38] H. Freundlich, Über die Adsorption in Lösungen, *Zeitschrift Für Phys. Chemie*, 57 (1906) 385–470.
- [39] H. Freundlich, Of the adsorption of gases. Section II. Kinetics and energetics of gas adsorption, *Trans. Faraday Soc.*, 28 (1931) 195–201.
- [40] M.J. Temkin, V. Pyzhev, Recent modifications to Langmuir isotherms, *Acta Physicochim. URSS*, 12 (1940) 217–225.
- [41] Y. Kim, C. Kim, I. Choi, S. Rengaraj, J. Yi, Arsenic removal using mesoporous alumina prepared via a templating method, *Environ. Sci. Technol.*, 38 (2004) 924–931.
- [42] S. Lagergren, Zur theorie der sogenannten adsorption gelöster stoffe, *K. Sven. Vetenskapsakad. Handl.*, 24 (1898) 1–39.
- [43] Y. Ho, G. McKay, Pseudo-second order model for sorption processes, *Process Biochem.*, 34 (1999) 451–465.
- [44] W. Wang, G. Tian, D. Wang, Z. Zhang, Y. Kang, L. Zong, A. Wang, All-into-one strategy to synthesize mesoporous hybrid silicate microspheres from naturally rich red polygorskite clay as high-efficient adsorbents, *Sci. Rep.*, 6 (2016) 39599.

Supporting Information

S1. Measurements

The chemical component of the circulating fluidized bed fly ash was determined by X-ray fluorescence (XRF) method (PANalytical B.V., Almelo, Netherlands). The Si and Al concentrations of supernatant extracted from circulating fluidized bed fly ash were detected by inductively coupled plasma optical emission spectrometry (ICP-OES) method on a PerkinElmer Optima 8300 Spectrometer. The powder X-ray diffraction (XRD) was carried out on an X'Pert Pro X-ray diffractometer by using Cu-K α radiation with a wavelength of 1.54184 Å. Nitrogen adsorption–desorption measurement was performed on a Micromeritics TriStar II 3020 surface area and porosity analyzer (Micromeritics Instrument Corporation, USA) at 77 K. Before the measurement, the synthesized mesoporous adsorbent was degassed under vacuum at 120°C for 12 h. The specific surface area

was calculated through Brunauer–Emmett–Teller (BET) method, while the pore size distribution was determined using the Barrett–Joyner–Halenda (BJH) model. The Fourier transform infrared (FT-IR) spectrum was collected on a Spectrum One Fourier transform infrared spectrometer (PerkinElmer Instruments Co. Ltd., USA) in the range of 4,000–450 cm⁻¹ using KBr as standard reference. The solid-state ²⁷Al MAS NMR spectrum was collected on a Bruker AVANCE III 400 spectrometer (Karlsruhe, Germany) using 1 M Al(NO₃)₃ solution as the reference. The TEM images of the starting fly ash and synthesized mesoporous adsorbent were obtained on a JEM 1200EX microscope (JEOL, Japan) operated at an accelerating voltage of 120 kV. A UV-5100 spectrophotometer (Shanghai Metash Instrument Co. Ltd., China) was used to analyze the concentration of malachite green (MG) solution.



Fig. S1. TEM image of as-received circulating fluidized bed fly ash.

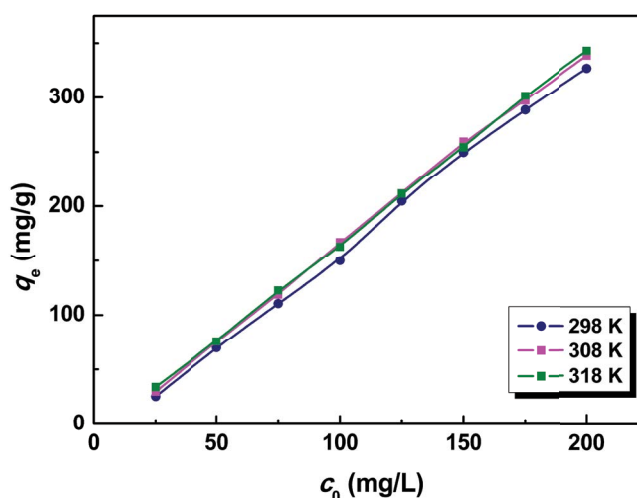


Fig. S2. Influence of initial MG concentrations onto equilibrium adsorption capacity at three temperatures.